nature microbiology

SUPPLEMENTARY INFORMATION

https://doi.org/10.1038/s41564-017-0059-5

In the format provided by the authors and unedited.

Corrected: Publisher correction

EphA2 is an epithelial cell pattern recognition receptor for fungal β-glucans

Marc Swidergall[1], Norma V. Solis[1], Michail S. Lionakis[2] and Scott G. Filler[1,3]*

[1]Division of Infectious Diseases, Los Angeles Biomedical Research Institute at Harbor-UCLA Medical Center, Torrance, CA, USA. [2]National Institute of Allergy and Infectious Diseases, National Institutes of Health, Fungal Pathogenesis Unit, Laboratory of Clinical Infectious Diseases, Bethesda, MD, USA. [3]David Geffen School of Medicine at UCLA, Los Angeles, CA, USA. *e-mail: sfiller@ucla.edu

nature microbiology

SUPPLEMENTARY INFORMATION

https://doi.org/10.1038/s41564-017-0059-5

In the format provided by the authors and unedited.

EphA2 is an epithelial cell pattern recognition receptor for fungal β-glucans

Marc Swidergall[1], Norma V. Solis[1], Michail S. Lionakis[2] and Scott G. Filler[1,3]*

[1]Division of Infectious Diseases, Los Angeles Biomedical Research Institute at Harbor-UCLA Medical Center, Torrance, CA, USA. [2]Fungal Pathogenesis Unit, Laboratory of Clinical Infectious Diseases, National Institute of Allergy and Infectious Diseases, National Institutes of Health, Bethesda, MD, USA. [3]David Geffen School of Medicine at UCLA, Los Angeles, CA, USA. *e-mail: sfiller@ucla.edu

EphA2 is an epithelial cell pattern recognition receptor for fungal β-glucans

Authors: Marc Swidergall, Norma V. Solis, Michail S. Lionakis, and Scott G. Filler

Supplementary Materials:
Tables S1-S3
Supplementary Figures 1-34

Table S1 Effect of EphA2 inhibitors on fungal growth

Phenotype	Ctrl	DAS	ANT
Mean doubling time	100% ± 4.17	95.69% ± 6.71	94.62% ± 10.37
Hyphal length	25.36 µm ± 7.16	23.42 µm ± 9.43	24.01 µm ±8.73

Table S2 Strains used in this study

Strain	Reference
C. albicans SC5314	[1]
C. albicans CAI4-GFP	[2]
C. albicans 529L	[3]
C. albicans efg1/cph1	[4]
C. albicans als3/ssa1	[5]
C. albicans ece1	[6]
C. glabrata 05-761	[7]
S. cerevisiae BY4743	[8]
R. delemar 99-880	[9]
A. fumigatus Af293	[10]
E. coli K12	[11]
S. aureus SH1000	[12]

Table S3 Oligonucleotides for RT-PCR

Oligonucleotide	Sequence
mIL23p19 Fwd	TGTGCCCCGTATCCAGGT
mIL23p19 Rev	CGGATCCTTTGCAAGCAGAA
mCRAMP Fwd	AGGAGATCTTGGGAACCATGCAGTT
mCRAMP Rev	GCAGATCTACTGCTCCGGCTGAGGTA
mTNFa Fwd	TACAGGCTTGTCACTCGAATT
mTNFa Rev	ATGAGCACAGAAAGCATGATG
mIL21 Fwd	GCCAGATCGCCTCCTGATTA
mIL21 Rev	CATGCTCACAGTGCCCCTTT
mIL5 Fwd	TCACCGAGCTCTGTTGACAA
mIL5 Rev	CCACACTTCTCTTTTTGGCG
KC Fwd	CCACCCGCTCGCTTCTC
KC Rev	CACTGACAGCGCAGCTCATT
mCxcl2 Fwd	CCTGCCAAGGGTTGACTTCA
mCxcl2 Rev	TTCTGTCTGGGCGCAGTG
mGm-csf Fwd	AGAAGCCCTGAACCTCCTGGATG
mGm-csf Rev	CCTGGGAACAACCCAACTCTCT
mTgfb Fwd	ACCGCAACAACGCCATCTAT
mTgfb Rev	GTAACGCCAGGAATTGTTGC
mIFNg Fwd	GCTCTGAGACAATGAACGCT
mIFNg Rev	AAAGAGATAATCTGGCTCTGC
mIL10 Fwd	ACTGCTATGCTGCCTGCTCTTACT
mIL10 Rev	GAATTCAAATGCTCCTTGATTTCT
mIL17c Fwd	ACCGCAATGAAGACCCTGAT
mIl17c Rev	TCCCTCCGCATTGACACA
mCcl3 Fwd	CTGCAACCAAGTCTTCTCAGC
mCcl3 Rev	CTGCCTCCAAGACTCTCAGG
Defb3 Fwd	GCTAGGGAGCACTTGTTTGC
Defb3 Rev	TTGTTTGAGGAAAGGAGGCA
mS100a8 Fwd	CCCGTCTTCAAGACATCGTTTG
mS100a8 Rev	ATATCCAGGGACCCAGCCCTAG
mIL17a Fwd	GGACTCTCCACCGCAATGA
mIl17a Rev	GGCACTGAGCTTCCCAGATC
mIL22 Fwd	CATGCAGGAGGTGGTACCTT
mIL22 Rev	CAGACGCAAGCATTTCTCAG
mGAPDH Fwd	CCTCGTCCCGTAGACAAAATG
mGAPDH Rev	TCTCCACTTTGCCACTGCAA
hIL8 Fwd	TCTGCAGCTCTGTGTGAAGG
hIL8 Rev	ACTTCTCCACAACCCTCTGC
hS100a8 Fwd	CCGAGTGTCCTCAGTATATCAGGA
hS100a8 Rev	GGCCATCTTTATCACCGAATGA
hCCL3 Fwd	CTTGGGTTGTGGAGTGAG
hCCL3 Rev	ACTGAAGCTCGTATCTC
hCCL20 Fwd	CTGGCTGCTTTGATGTCAGT
hCCL20 Rev	CGTGTGAAGCCCACAATAAA
hGAPDH Fwd	CCACTCCTCCACCTTTGAC
hGAPDH Rev	ACCCTGTTGCTGTAGCCA

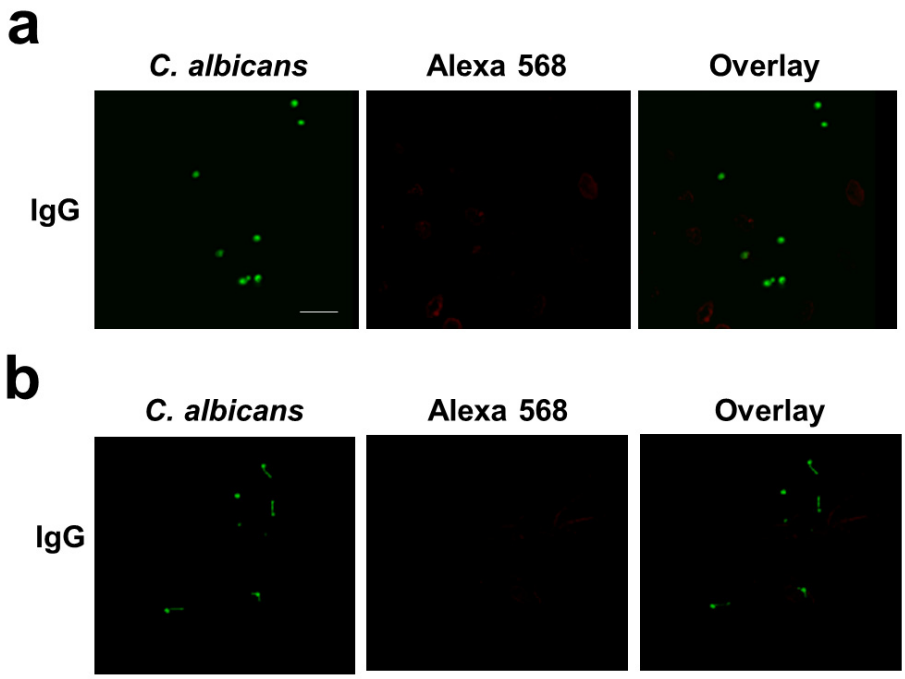

Supplementary Figure 1 IgG control staining during *C. albicans* infection of oral epithelial cells. (**a**) Yeast or (**b**) hyphae *C. albicans* expressing GFP (CAI4-GFP) 15 or 90 min post infection of oral epithelial cells. Samples were incubated with IgG control, followed by anti-rabbit-Alexa 568 Ab. Results are representative of 3 independent experiments. Scale bar 20 μm.

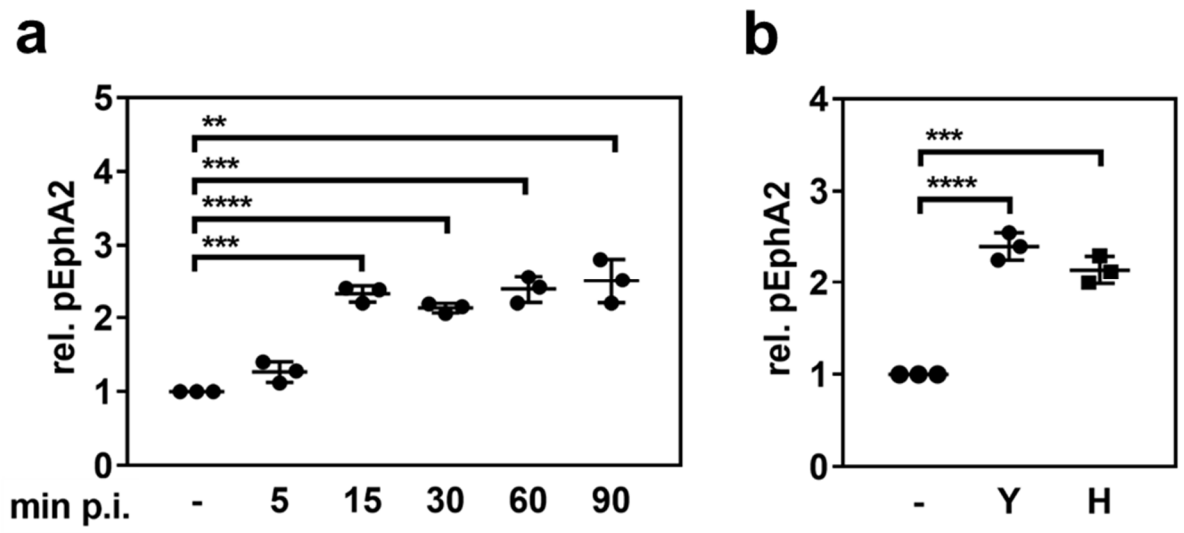

Supplementary Figure 2 Densitometric analysis of EphA2 phosphorylation during *C. albicans* infection of oral epithelial cells. (**a**) EphA2 phosphorylation in oral epithelial cells infected with yeast-phase *C. albicans* SC5314 for the indicated times. (**b**) EphA2 phosphorylation in epithelial cells exposed to either yeast-phase or hyphal-phase *C. albicans* for 20 min. Graphs show the relative ratio of phosphorylated EphA2 to total EphA2. Data are the mean ± SD of 3 independent immunoblots. Images of representative immunoblots are show in Fig. 1c, d). H, hyphae; p.i., post-infection; Y, yeast. $^{**}P < 0.01$, $^{***}P < 0.001$, $^{****}P < 0.0001$ (two-tailed Student's t-test assuming unequal variances).

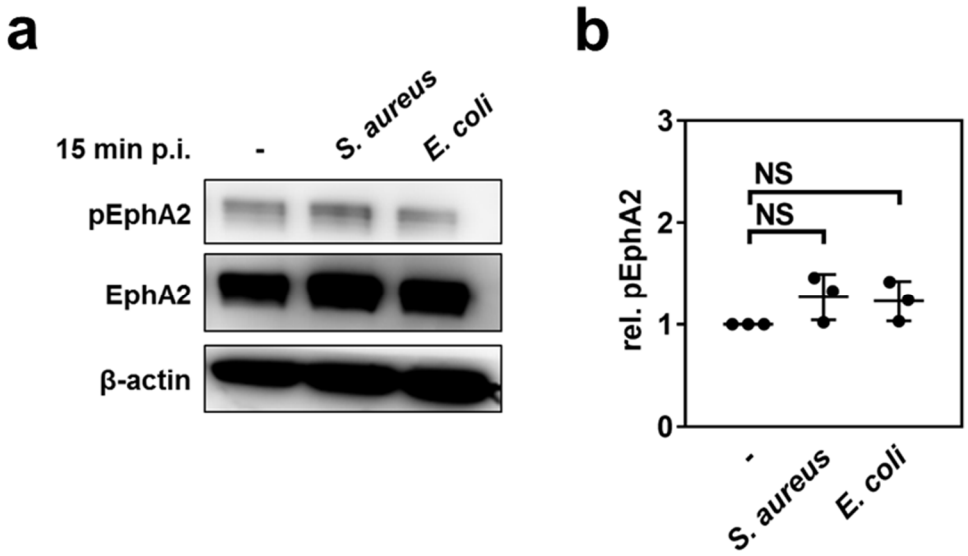

Supplementary Figure 3 EphA2 is not activated by epithelial cell infection with *Staphylococcus aureus* or *Escherichia coli*. (**a**) Immunoblot showing EphA2 phosphorylation of epithelial cells after 15 min infection with *S. aureus* SH1000 and *E. coli* K12 at multiplicity of infection of 5 organisms per epithelial cell. (**b**) Densitometric analysis of immunoblots as in (**a**). Data are the mean ± SD of 3 independent immunoblots. NS, not significant (two-tailed Student's t-test assuming unequal variances).

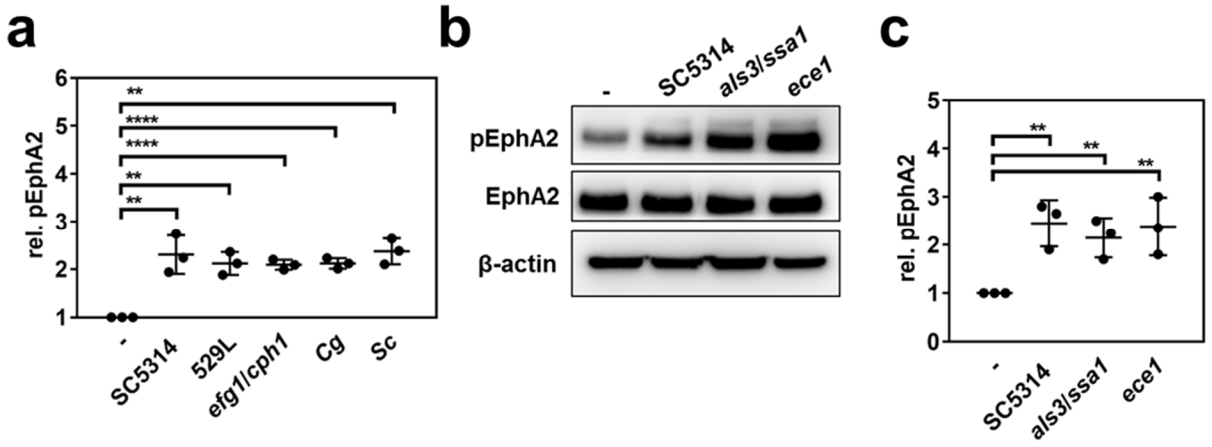

Supplementary Figure 4 Effects of different fungal strains on EphA2 phosphorylation. (**a**) *C. albicans* (SC5314, 529L, *efg1/cph1*), *Candida glabrata*, and *Saccharomyces cerevisiae*. Image of a representative immunoblot is shown in Fig. 1e). (**b-c**) Immunoblot showing EphA2 phosphorylation of epithelial cells after 15 min infection with *C. albicans* (SC5314) or the indicated mutants (**c**) Densitometric analysis of immunoblots as in (**b**).. *Cg*, *C. glabrata*; *Sc*, *S. cerevisiae*. Data are the mean ± SD of 3 independent immunoblots. $^{**}P < 0.01$, $^{****}P < 0.0001$ (two-tailed Student's t-test assuming unequal variances).

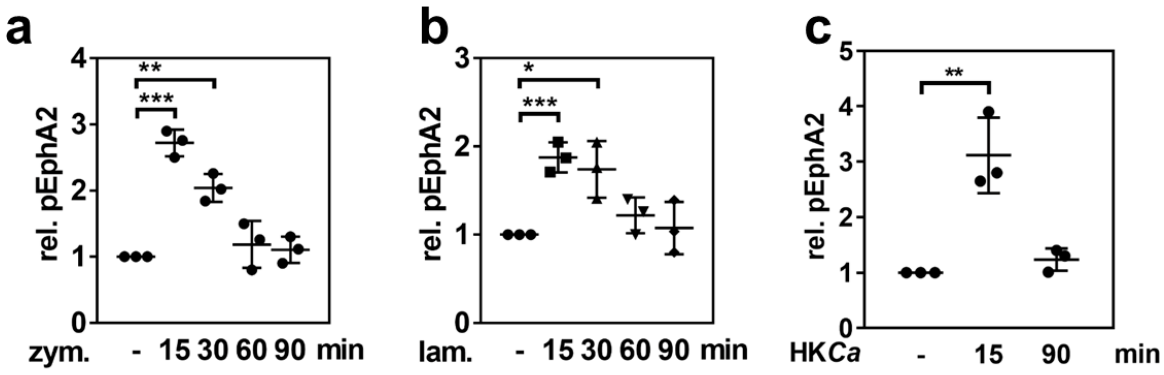

Supplementary Figure 5 Densitometric analysis of EphA2 phosphorylation induced by heat-killed *C. albicans* and the β-glucans zymosan and laminarin. EphA2 phosphorylation in epithelial cells that were incubated for the indicated times with (**a**) zymosan (50 µg/ml), (**b**) laminarin (50 µg/ml) and (**c**) heat-killed *C. albicans* yeast (5 organisms per epithelial cell). Data are the mean ± SD of 3 independent immunoblots. Images of representative immunoblots are shown in Fig. 1f-g). HK*Ca*, heat-killed *C. albicans*; lam, laminarin; zym, zymosan. **P* < 0.05, ***P* < 0.01, ****P* < 0.001 (two-tailed Student's t-test assuming unequal variances).

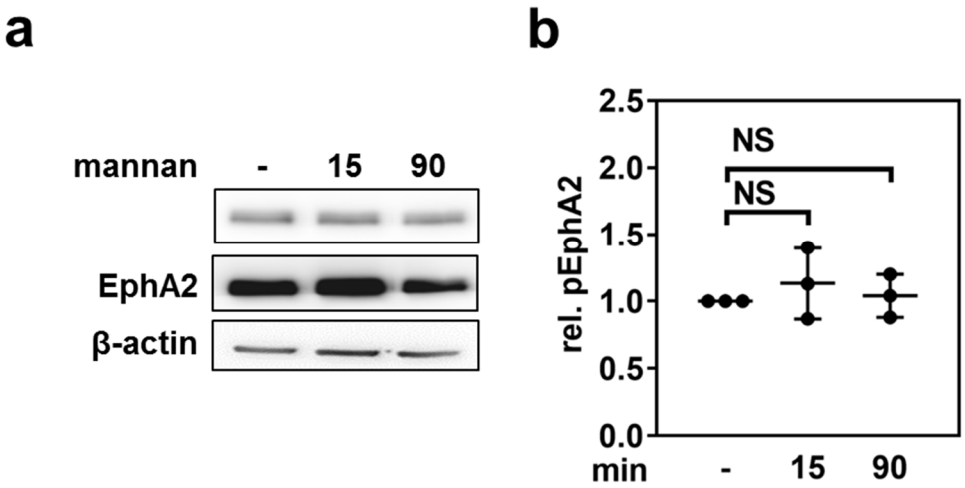

Supplementary Figure 6 Mannan does not activate EphA2. Extent of EphA2 phosphorylation in epithelial cells that were incubated for 15 and 90 min with mannan (50µg/mL). (**a**) Representative immunoblots. (**b**) Densitometric analysis. Data are the mean ± SD of 3 independent immunoblots. NS, not significant (two-tailed Student's t-test assuming unequal variances).

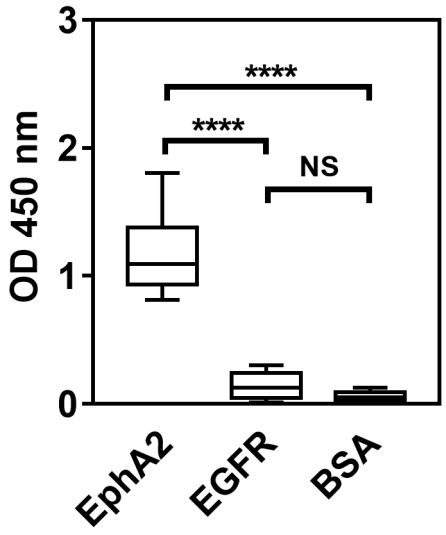

Supplementary Figure 7 EGFR does not bind to β-glucan. Binding of recombinant EphA2, the epidermal growth factor receptor and BSA to immobilized zymosan, as determined by ELISA. Box whisker plots show median and range of 3 experiments, each performed in triplicate. EGFR, epidermal growth factor receptor. ****$P < 0.0001$; NS, not significant (two-tailed Student's t-test assuming unequal variances).

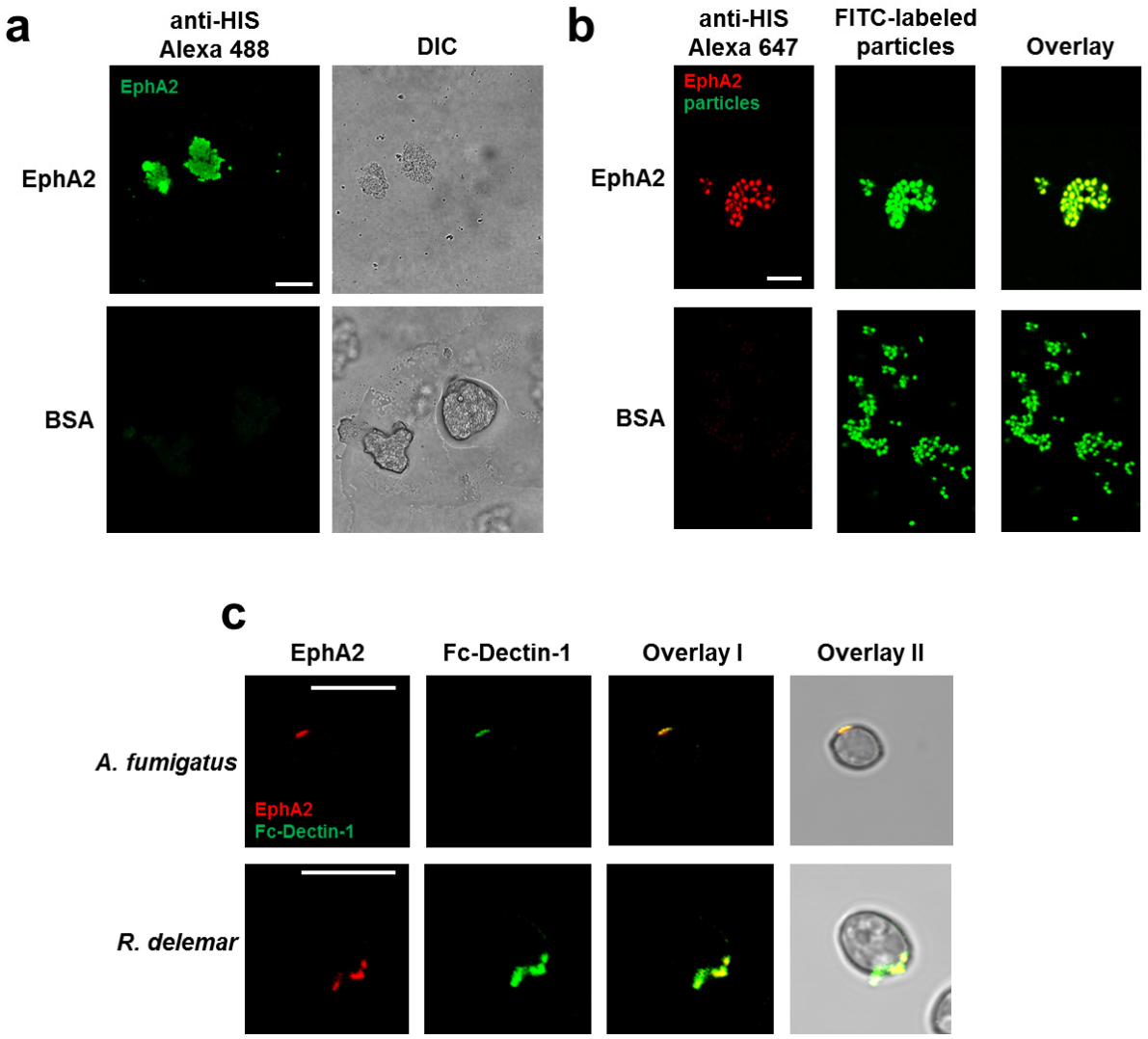

Supplementary Figure 8 EphA2 binds β-glucan. (**a**) EphA2 (green) binding to zymosan coated coverslips. Scale bar 50 µm. (**b**) EphA2 binding (red) to FITC coated zymosan bioparticles (green). Scale bar 20 µm. (**c**) EphA2 and dectin-1-Fc co-localize on the surface of swollen spores and conidia of filamentous fungi. Images of swollen conidia of *Aspergillus fumigatus* and *Rhizopus delemar* that were stained with recombinant EphA2 (red) and Fc-Dectin-1 (green). Results are representative of 3 independent experiments. Scale bar 10 µm.

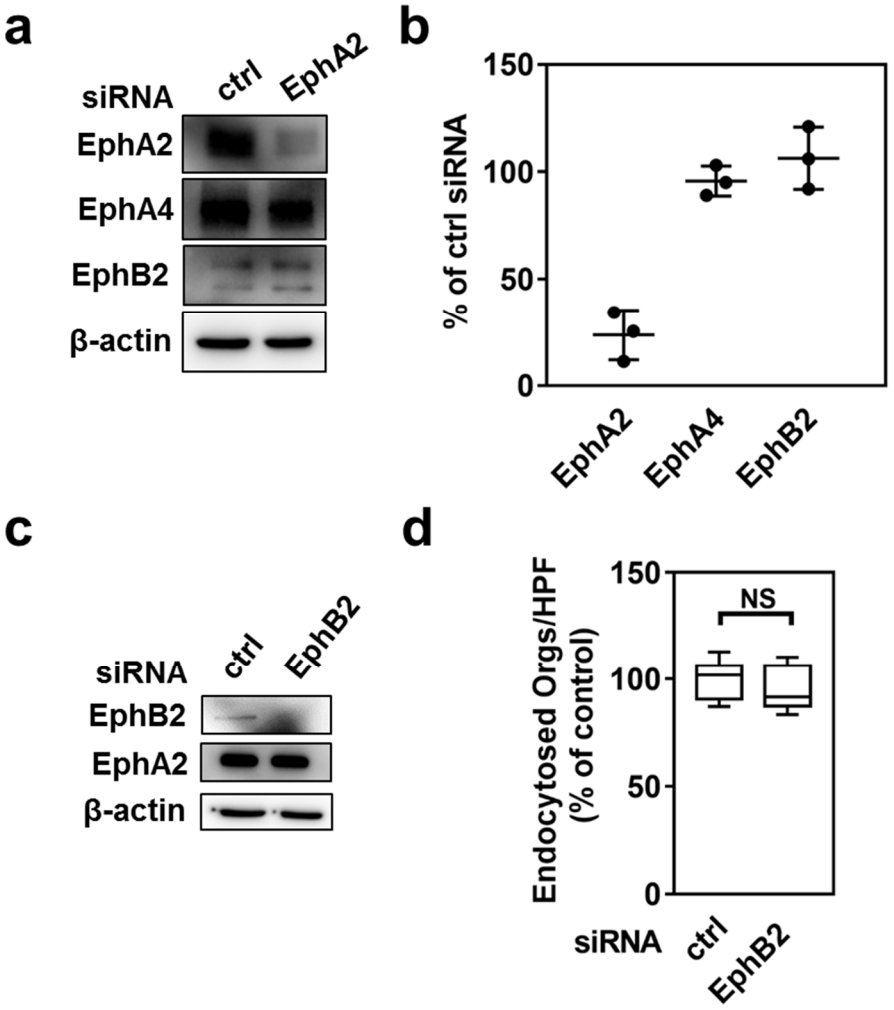

Supplementary Figure 9 EphA2 depletion in oral epithelial cells does not affect expression of related ephrin receptors. (**a**) Representative immunoblots showing EphA2, EphA4, and EphB2 levels in epithelial cells that had been transfected with EphA2 siRNA. (**b**) Densitometric analysis of the immunoblots such as in (**a**). Results are the mean ± SD of 3 independent immunoblots. (**c**) EphB2 depletion has no effect on epithelial cells EphA2 levels. Representative immunoblot of EphB2 depletion in oral epithelial cells. (**d**) Depletion of EphB2 with siRNA has no effect on the endocytosis of *C. albicans*. Box whisker plots show median and range ± SD of 2 independent experiments, each performed in triplicate. NS, not significant (two-tailed Student's t-test assuming unequal variances).

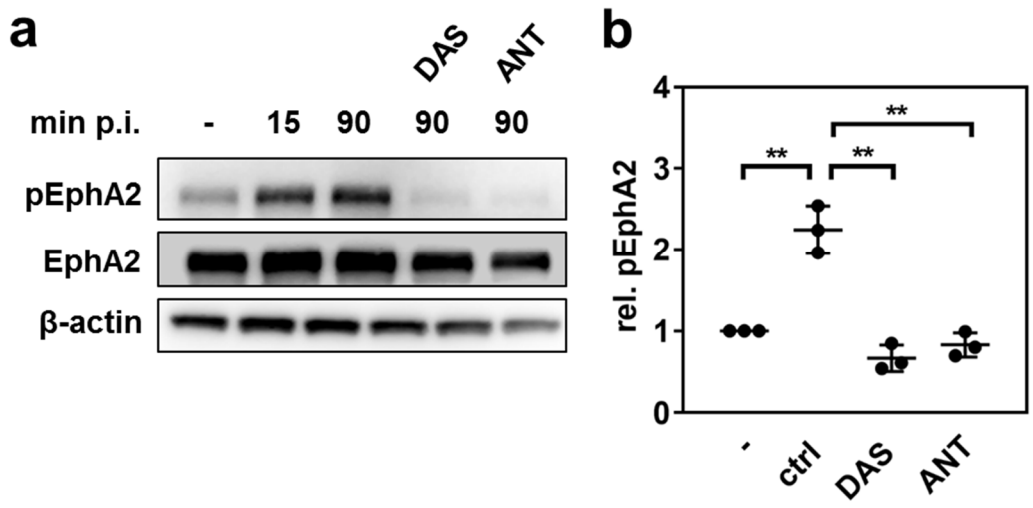

Supplementary Figure 10 EphA2 inhibitors block *C. albicans*-induced EphA2 activation. EphA2 phosphorylation in oral epithelial cells that were preincubated with dasatinib or an EphA2 antagonist and then infected with *C. albicans*. (**a**) Representative immunoblots. (**b**) Densitometric analysis of EphA2 phosphorylation after 90 min of *C. albicans* exposure. Results are the mean ± SD of 3 independent immunoblots. Ctrl, control; DAS, dasatinib; ANT, EphA2 antagonist. ***P* < 0.01 (two-tailed Student's t-test assuming unequal variances).

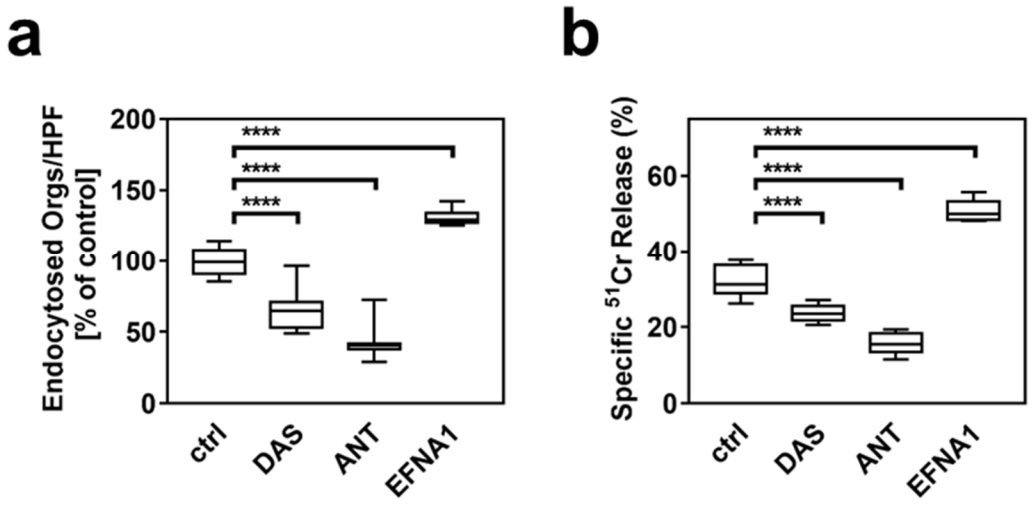

Supplementary Figure 11 Inhibition of EphA2 reduces *C. albicans* endocytosis and epithelial cell damage. Effects of treatment of oral epithelial cells with DAS, ANT or ephrin A1 on the endocytosis of *C. albicans* (**a**) and extent of *C. albicans*-induced epithelial cell damage (**b**). Box whisker plots show median and range ± SD of 3 independent experiments, each performed in triplicate. Ctrl, control. ANT, EphA2 antagonist; DAS, dasatinib; EFNA1, ephrin A1. ****$P <$ 0.0001 (two-tailed Student's t-test assuming unequal variances).

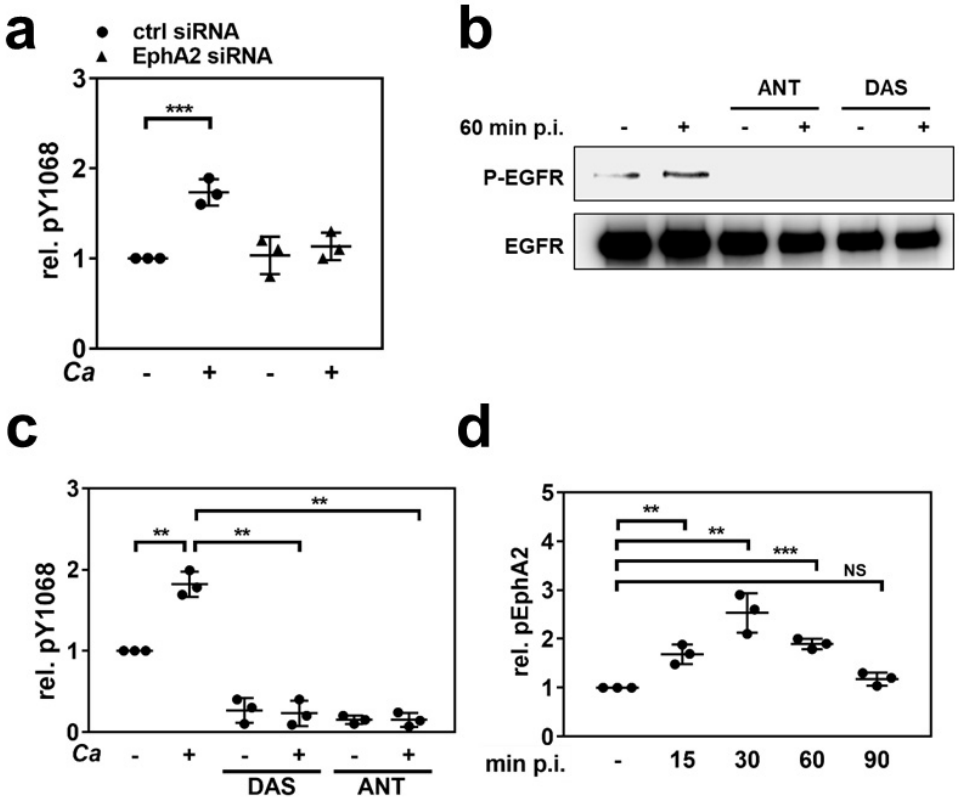

Supplementary Figure 12 EphA2 and the epidermal growth factor receptor (EGFR) act in the same pathway during *C. albicans* infection. (**a**) Densitometric analysis of EGFR Y1068 phosphorylation after 60 min of *C. albicans* infection in epithelial cells that had been transfected with EphA2 siRNA. Results are the mean ± SD of 3 independent immunoblots. Representative immunoblot is shown in Fig. 2d. (**b, c**) EGFR phosphorylation at Y1068 in oral epithelial cells that had been pre-treated for 1 h with EphA2 inhibitors (DAS and ANT) and then infected for 60 min with *C. albicans*. (**b**) Representative immunoblot. (**c**) Densitometric analysis. Data are the mean ± SD of 3 independent immunoblots. (**d**) Densitometric analysis of EphA2 phosphorylation in oral epithelial cells treated with the EGFR inhibitor gefitinib. Representative immunoblot is shown in Fig. 2e. Ctrl, control. ANT, EphA2 antagonist; DAS, dasatinib. **P* < 0.05, ***P* < 0.01, ****P* < 0.001, *****P* < 0.0001 (two-tailed Student's t-test assuming unequal variances).

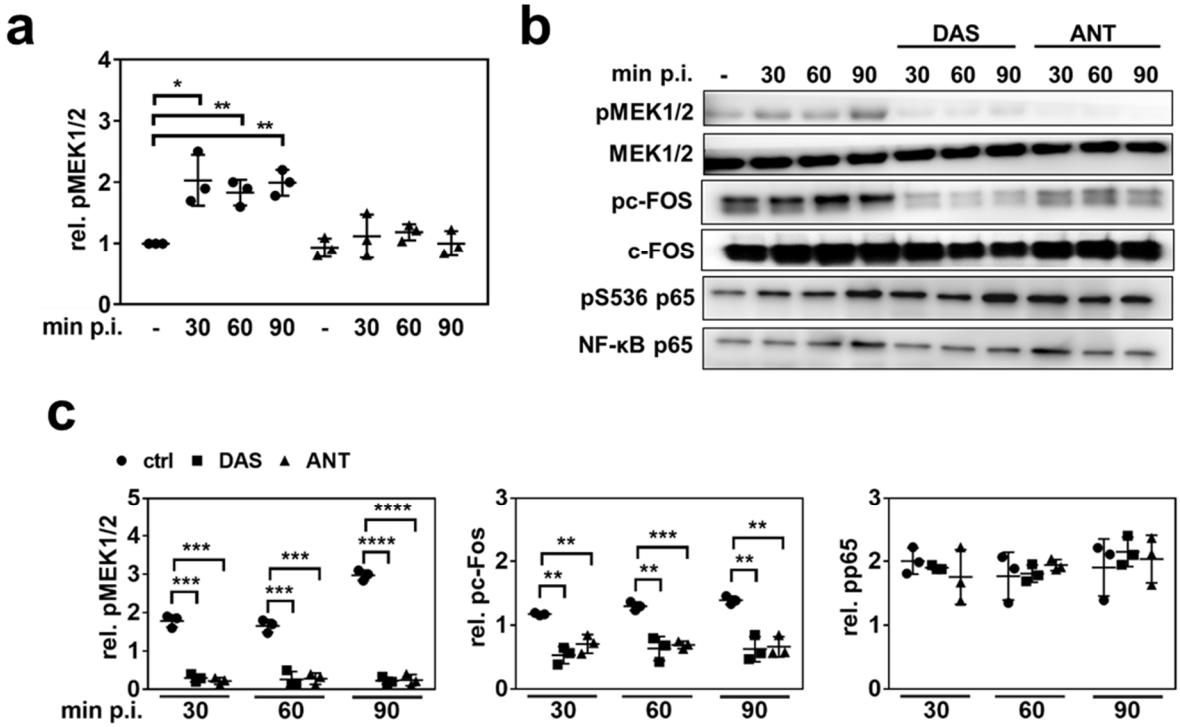

Supplementary Figure 13 Effects of EphA2 depletion and inhibition on phosphorylation of MEK1/2, c-Fos, and p65. (**a**) Densitometric analysis of MEK1/2 phosphorylation after 60 min of *C. albicans* exposure epithelial cells transfected with EphA2 siRNA. Representative immunoblot is shown in Fig. 2f. (**b, c**) Effects of DAS and ANT on the phosphorylation of epithelial cell MEK1/2, c-FOS, and S536 of NF-κB p65 in response to *C. albicans* infection. (**b**) Representative immunoblot (**c**) Densitometric analysis. Data are the mean ± SD of the densitometric analysis of 3 independent immunoblots. ANT, EphA2 antagonist; DAS, dasatinib. $^{**}P < 0.01$, $^{***}P < 0.001$, $^{****}P < 0.0001$ (two-tailed Student's t-test assuming unequal variances).

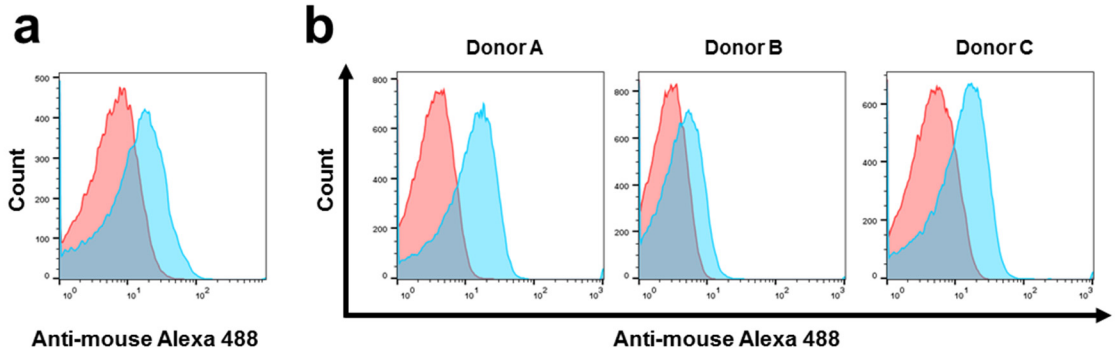

Supplementary Figure 14 Dectin-1 is expressed on the surface of human oral epithelial cells. Flow cytometric analysis of dectin-1 surface expression on (**a**) the OKF6/TERT-2 human epithelial cell line and (**b**) human buccal epithelial cells from 3 different donors from a single experiment. Histograms from OKF6/TERT-2 or human buccal epithelial cells stained with the control IgG are shown in red and results from cells stained with the dectin-1 antibody are shown in blue.

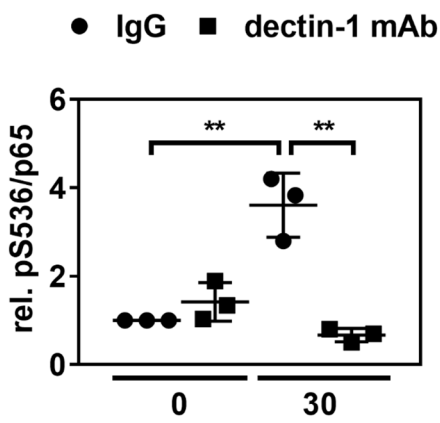

Supplementary Figure 15 Densitometric analysis of NF-κB p65 phosphorylation. Oral epithelial cells were pretreated with control IgG or a dectin-1 mAb, and then infected with *C. albicans*. Data are the mean ± SD of 3 independent immunoblots. Representative immunoblot is shown in Fig. 2g. $^{**}P < 0.01$ (two-tailed Student's t-test assuming unequal variances).

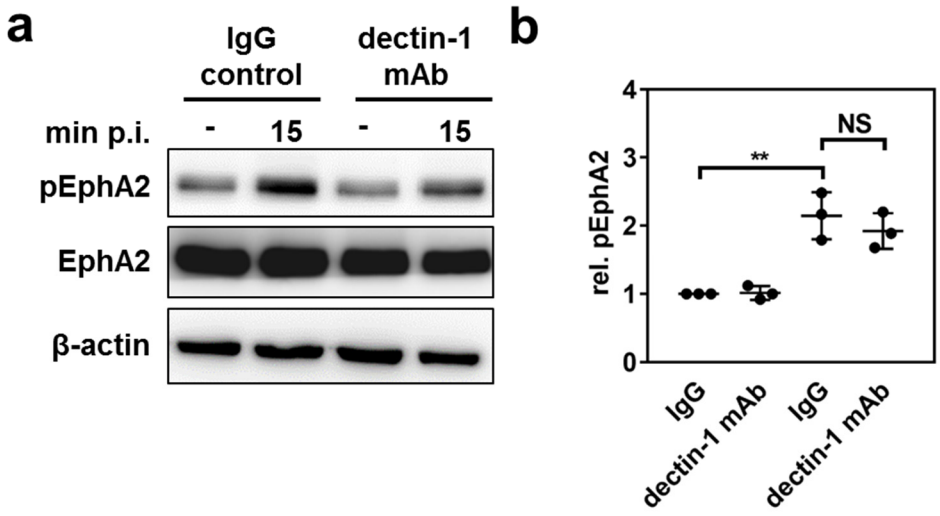

Supplementary Figure 16 EphA2 phosphorylation is independent of dectin-1 signaling in human oral epithelial cells. (**a**) Representative immunoblot showing EphA2 phosphorylation in epithelial cells that were pre-treated with control IgG or a dectin-1 neutralizing antibody for 1 h prior to *C. albicans* infection. (**b**) Densitometric analysis of immunoblots such as the one in (**A**). Data are the mean ± SD of 3 independent immunoblots. $^{**}P < 0.01$; NS, not significant (two-tailed Student's t-test assuming unequal variances).

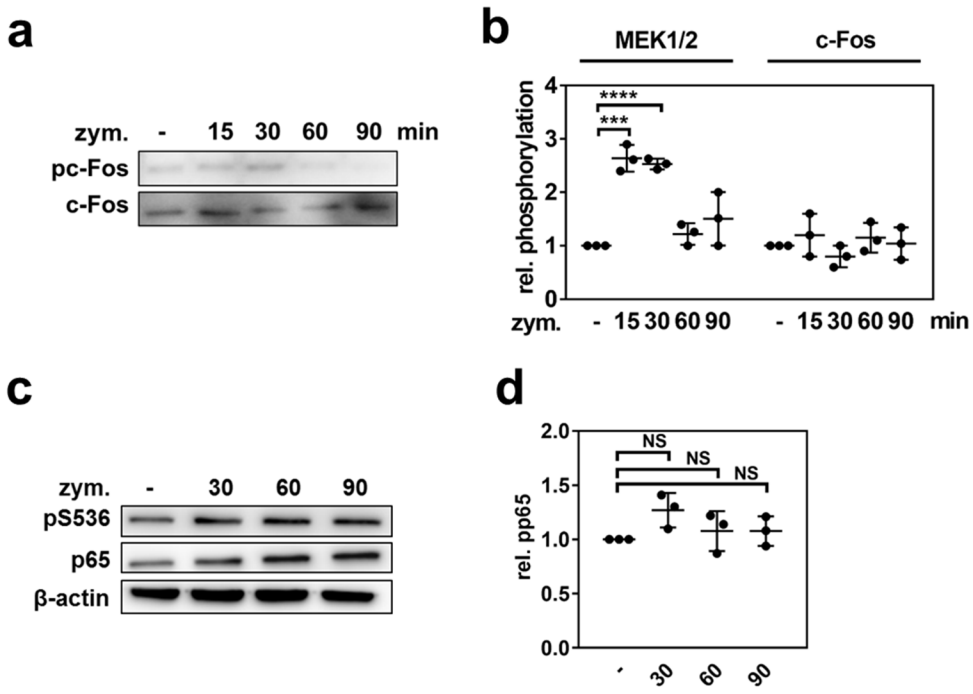

Supplementary Figure 17 Zymosan induces transient MEK1/2 activation, but has no effect on c-Fos and p65 activation. (**a**) Representative immunoblot showing the phosphorylation of c-Fos in oral epithelial cells that had been incubated with zymosan (50 μg/mL) for the indicated time. (**b**) Densitometric analysis of MEK1/2 and c-Fos phosphorylation incubated with zymosan. Data are the mean ± SD of 3 independent immunoblots. Representative immunoblot of showing MEK1/2 phosphorylation is show in Fig. 2h. (**c**) Representative immunoblot showing the phosphorylation of p65 of zymosan exposed oral epithelial cells. (**d**) Densitometric analysis of immunoblots such as the one in (**c**). Data are the mean ± SD of 3 independent immunoblots. ***P < 0.001, ****P < 0.0001, NS, not significant (two-tailed Student's t-test assuming unequal variances).

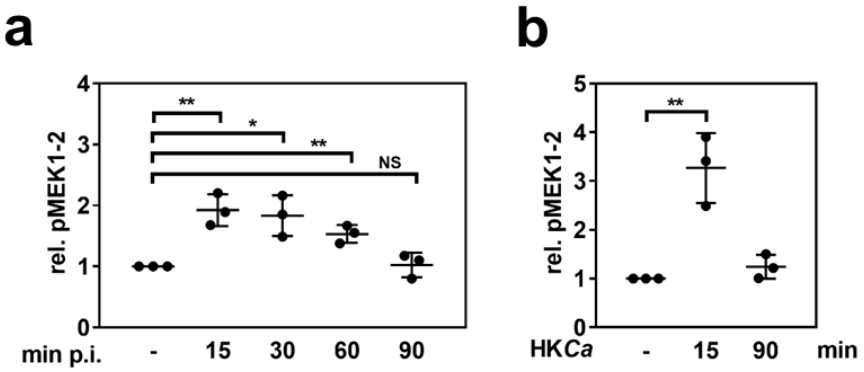

Supplementary Figure 18 EGFR signaling and viable organism are required to prolong MEK1/2 activation. (**a**) Densitometric analysis of immunoblots of MEK1/2 phosphorylation of oral epithelial cells treated with gefitinib (EGFR inhibitor). (**b**) Densitometric analysis of immunoblots of oral epithelial cells incubated with heat-killed *C. albicans*. Data are the mean ± SD of 3 independent immunoblots. Representative immunoblots are shown in Fig. 2i, j. HK*Ca*, heat-killed *C. albicans*. $^{**}P < 0.01$, $^{***}P < 0.001$ (two-tailed Student's t-test assuming unequal variances).

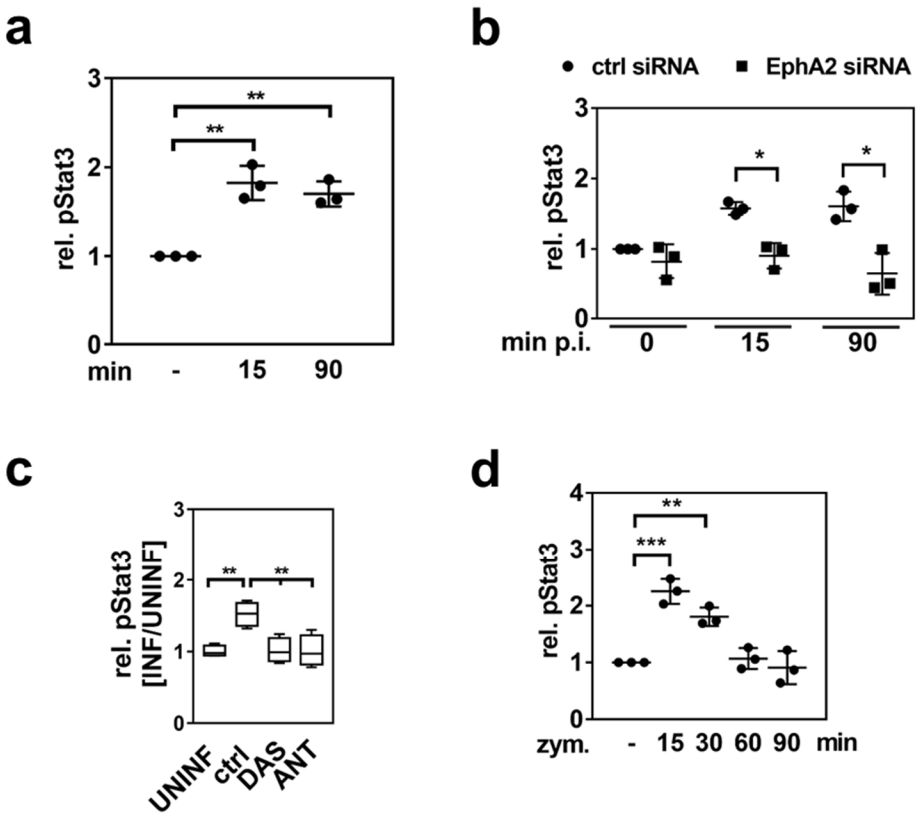

Supplementary Figure 19 Phosphorylation of Stat3. (**a**) Stat3 is activated during *C. albicans* infection. Densitometric analysis of immunoblots showing *C. albicans*-induced Stat3 phosphorylation. Data are the mean ± SD of 3 independent immunoblots. (**b**) Densitometric analysis of immunoblots of the effect of siRNA depletion of EphA2 on Stat3 phosphorylation in epithelial cells infected with *C. albicans*. Data are the mean ± SD of 3 independent immunoblots. (**c**) Effects of the EphA2 inhibitors, DAS and ANT on *C. albicans*-induced phosphorylation of Stat3, as measured by ELISA. Box whisker plots show median and range of 3 experiments, each performed in 3. (**d**) Densitometric analysis of zymosan-induced Stat3 phosphorylation. Data are the mean ± SD of 3 independent immunoblots. **P* < 0.05, ***P* < 0.01, ****P* < 0.001 (two-tailed Student's t-test assuming unequal variances).

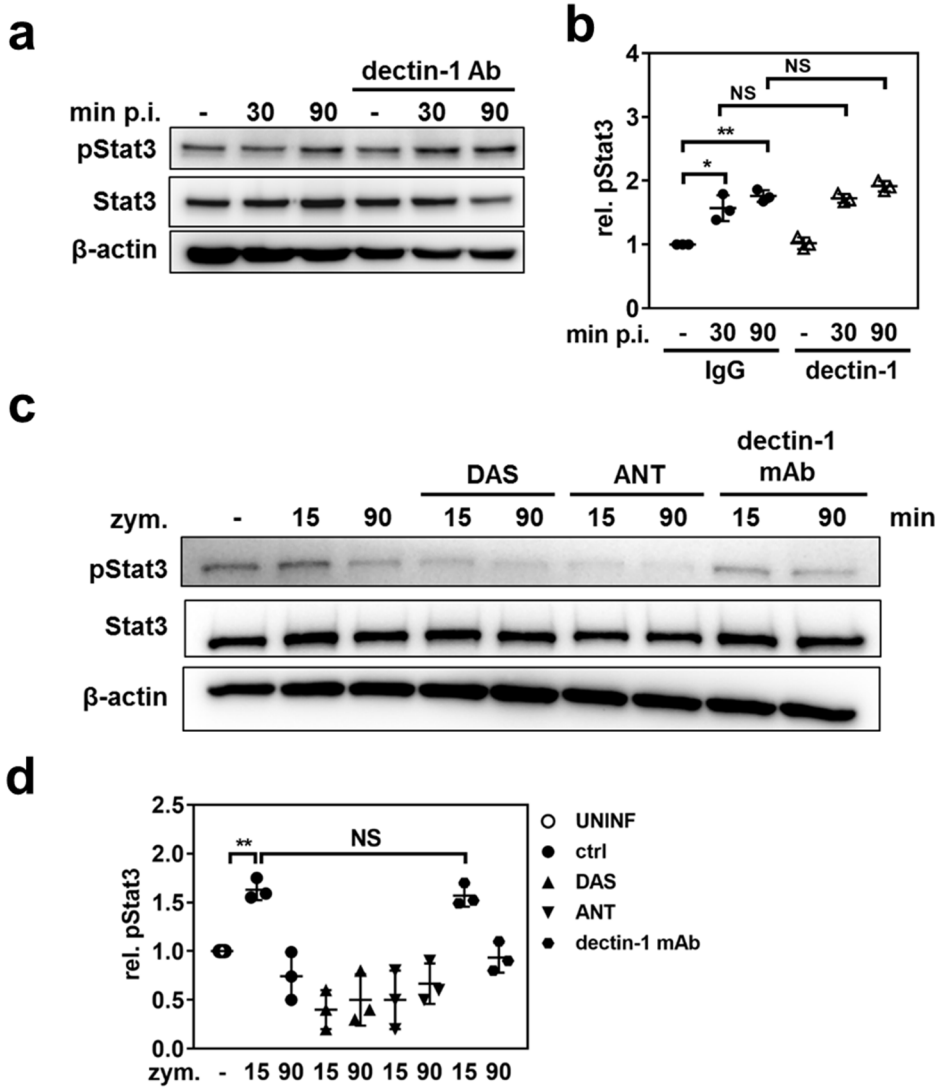

Supplementary Figure 20 Stat3 activation requires EphA2, but not dectin-1. (**a**-**b**) Stat3 phosphorylation in oral epithelial cells were incubated for 1 h with neutralizing anti-dectin-1 mAb, and then exposed to *C. albicans* for indicated times. (**a**) Representative immunoblot (**b**) Densitometric analysis. Data are the mean ± SD of 3 independent immunoblots. (**c-d**) Stat3 phosphorylation in oral epithelial cells were incubated for 1 h with DAS, ANT, or a neutralizing anti-dectin-1 mAb, and then exposed to zymosan for indicated times. (**c**) Representative immunoblot (**d**) Densitometric analysis. Data are the mean ± SD of 3 independent immunoblots. **P* < 0.05, ***P* < 0.01; NS; not significant (two-tailed Student's t-test assuming unequal variances).

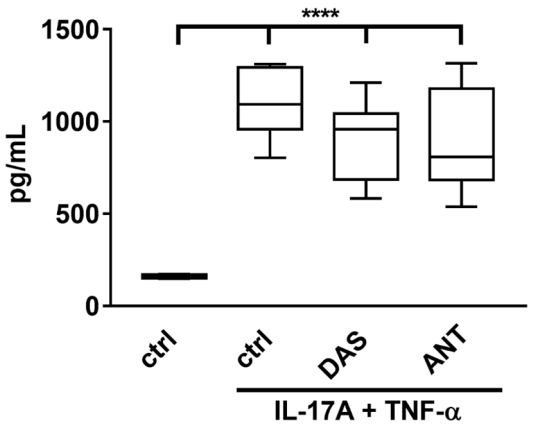

Supplementary Figure 21 EphA2 inhibition had no effect of secretion of IL-8 induced by IL-17A and TNF-α. IL-8 secretion by oral epithelial cells that were treated with DAS or ANT and then incubated for 20 h with IL-17A (50 ng/mL) and TNF-α (0.5 ng/mL). Box whisker plots show median and range of three independent experiments, each performed in duplicate. ****$P < 0.0001$ (two-tailed Student's t-test assuming unequal variances).

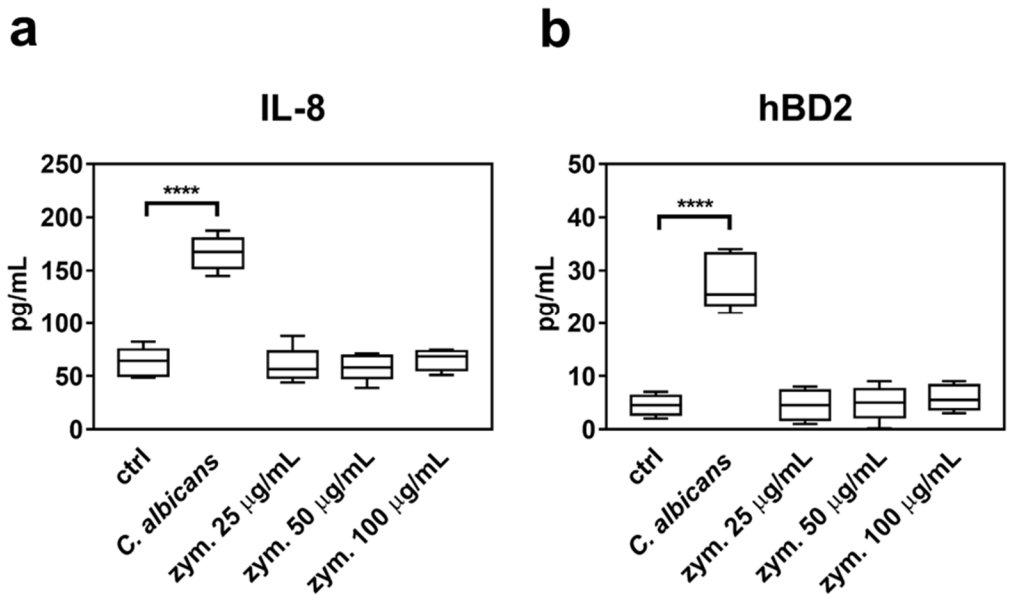

Supplementary Figure 22 Zymosan does not induces production of IL-8 or hBD2 by epithelial cells. Oral epithelial cells were incubated with *C. albicans* or the indicated concentrations of zymosan for 8 hours and the supernatant were analyzed for IL-8 (**a**) and hBD2 (**b**) content by ELISA. Box whisker plots show median and range of three independent experiments, each performed in duplicate. Zym, zymosan. ****$P < 0.0001$ (two-tailed Student's t-test assuming unequal variances).

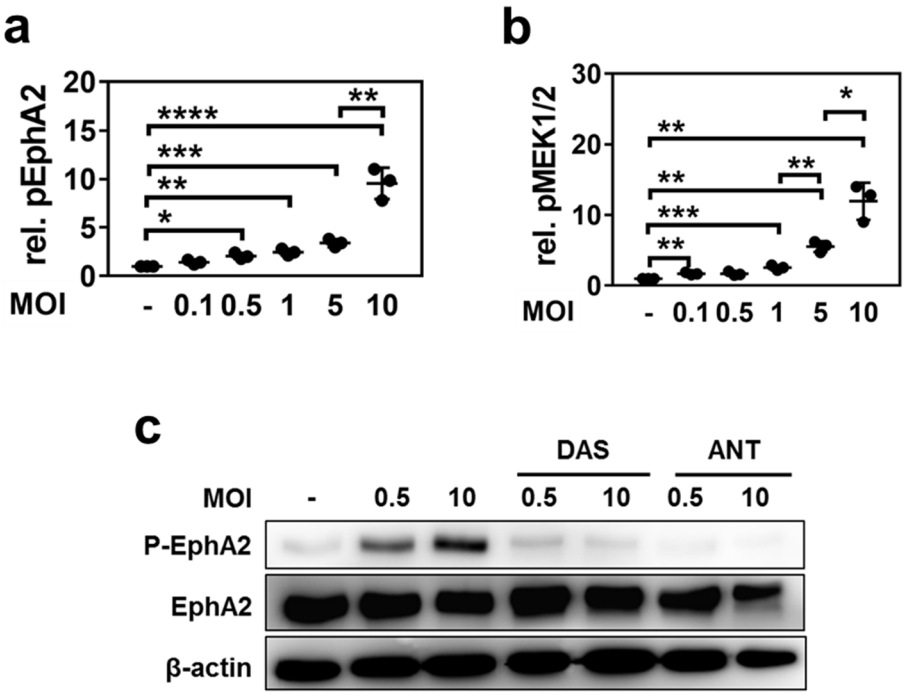

Supplementary Figure 23 Effects of *C. albicans* inoculum on the phosphorylation of EphA2 and MEK1/2. Densitometric analysis of the phosphorylation of (**a**) EphA2 and (**b**) MEK1/2 in oral epithelial cells that had been incubated for 30 min with *C. albicans* at the indicated multiplicities of infection (MOI). Data are the mean ± SD of 3 independent immunoblots. Representative immunoblots are shown in Fig 4a. **P* < 0.05, ***P* < 0.01, ****P* < 0.001, *****P* < 0.0001 (two-tailed Student's t-test assuming unequal variances). (**c**) DAS and ANT block *C. albicans*-induced phosphorylation of EphA2 at low and high MOIs. Representative immunoblots.

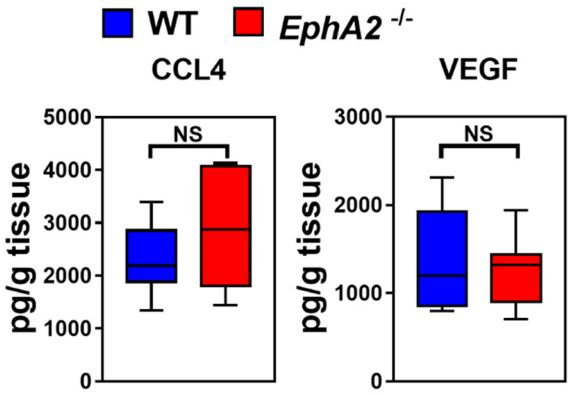

Supplementary Figure 24 Inflammatory mediator expression during OPC. Level of chemokines and cytokines in the tongue homogenates of immunocompetent wild-type and *EphA2*$^{-/-}$ mice with OPC after 1 d of infection. Box whisker plots show median and range of 4 mice in each group, tested in duplicate in a single experiment. NS, not significant (Mann-Whitney Test).

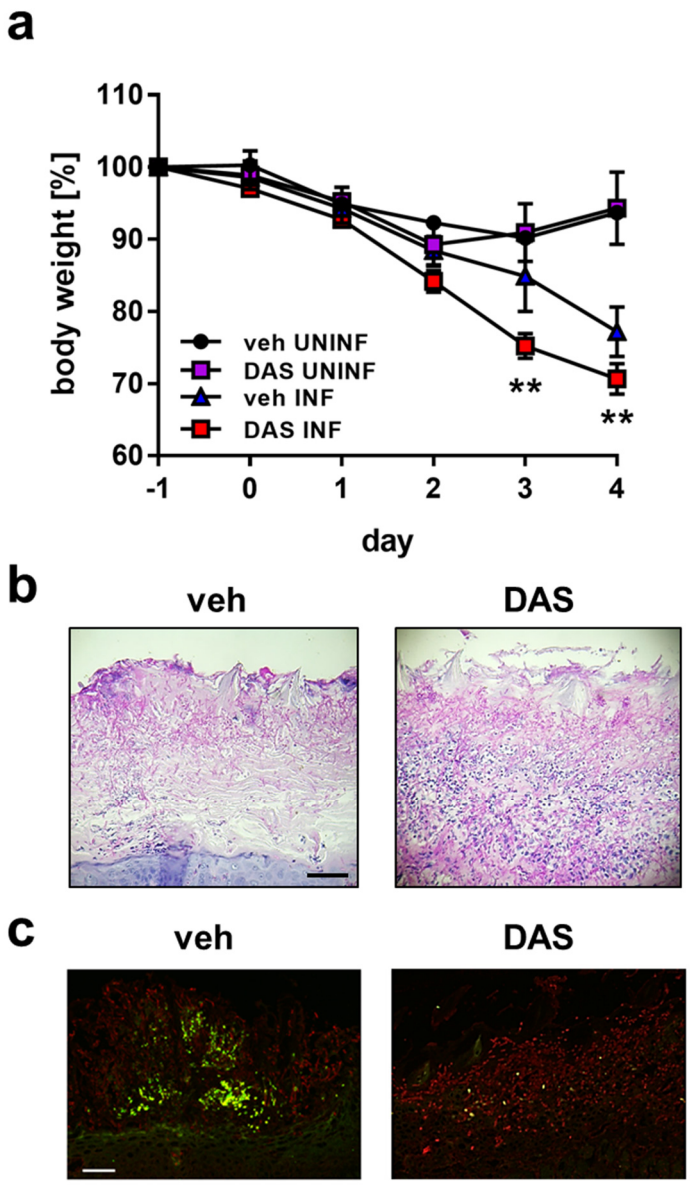

Supplementary Figure 25 Effect of dasatinib on body weight, fungal tissue invasion and Stat3 activation during OPC. Wild-type mice were immunosuppressed with triamcinolone (15mg/kg), treated with either DAS or the vehicle control, and orally inoculated with *C. albicans*. They were analyzed after 4 d of infection. (**a**) Body mass of mice with OPC. Results are the mean ± SD of 7 mice per group in a single experment. Results are mean ± SD. $^{**}P < 0.01$ (Holm-Sidak method). (**b**) Images f PAS-stained thin sections of the tongues of mice treated with the vehicle control or DAS after 4 d of infection. Results are representative of 3 mice in 2 independent experiments. Scale bar 100 µM. (**c**) Immunofluorescence images of the tongues of mice treated with the vehicle control or DAS after 4 d of infection. The tongues were stained with antibodies against phospho-Stat3 (green) and *C. albicans* (red). Scale bar 50 µm. DAS, dasatinib; Veh, vehicle; WT, wild type.

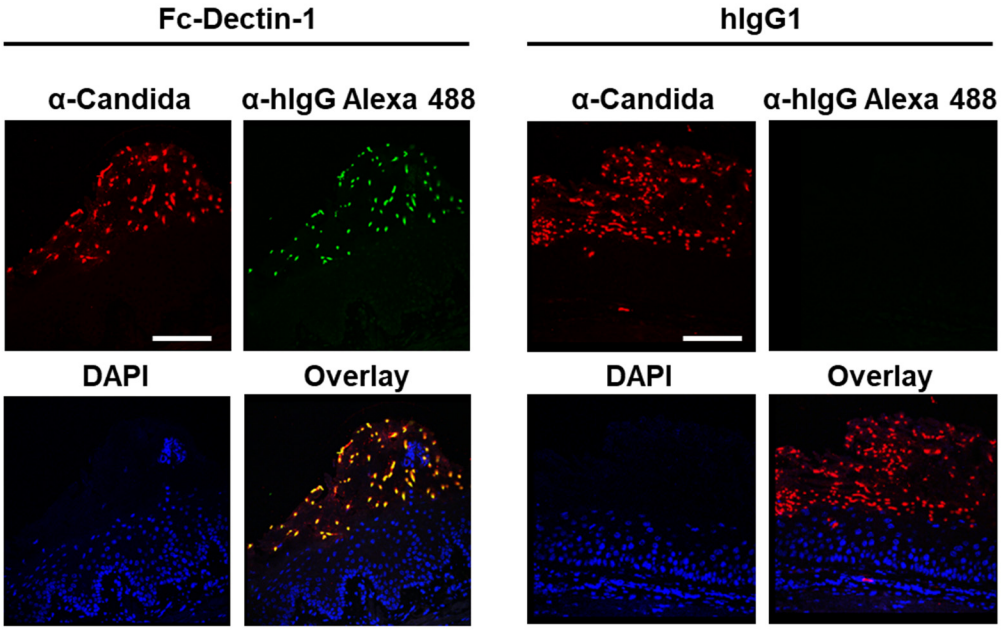

Supplementary Figure 26 β-glucan expression during OPC. Wild-type mice were immunosuppressed with triamcinolone (15mg/kg), treated with either DAS or the vehicle control, and orally inoculated with *C. albicans*. Immunofluorescence images of the tongues after 4 d of infection. The tongues were stained with antibodies against *Candida* (red), β-glucan (green) and host cells (blue). β-glucan staining was performed with Fc-Dectin-1 or control human IgG. Results are representative of 3 mice in a single experiment. Scale bar 100 μm.

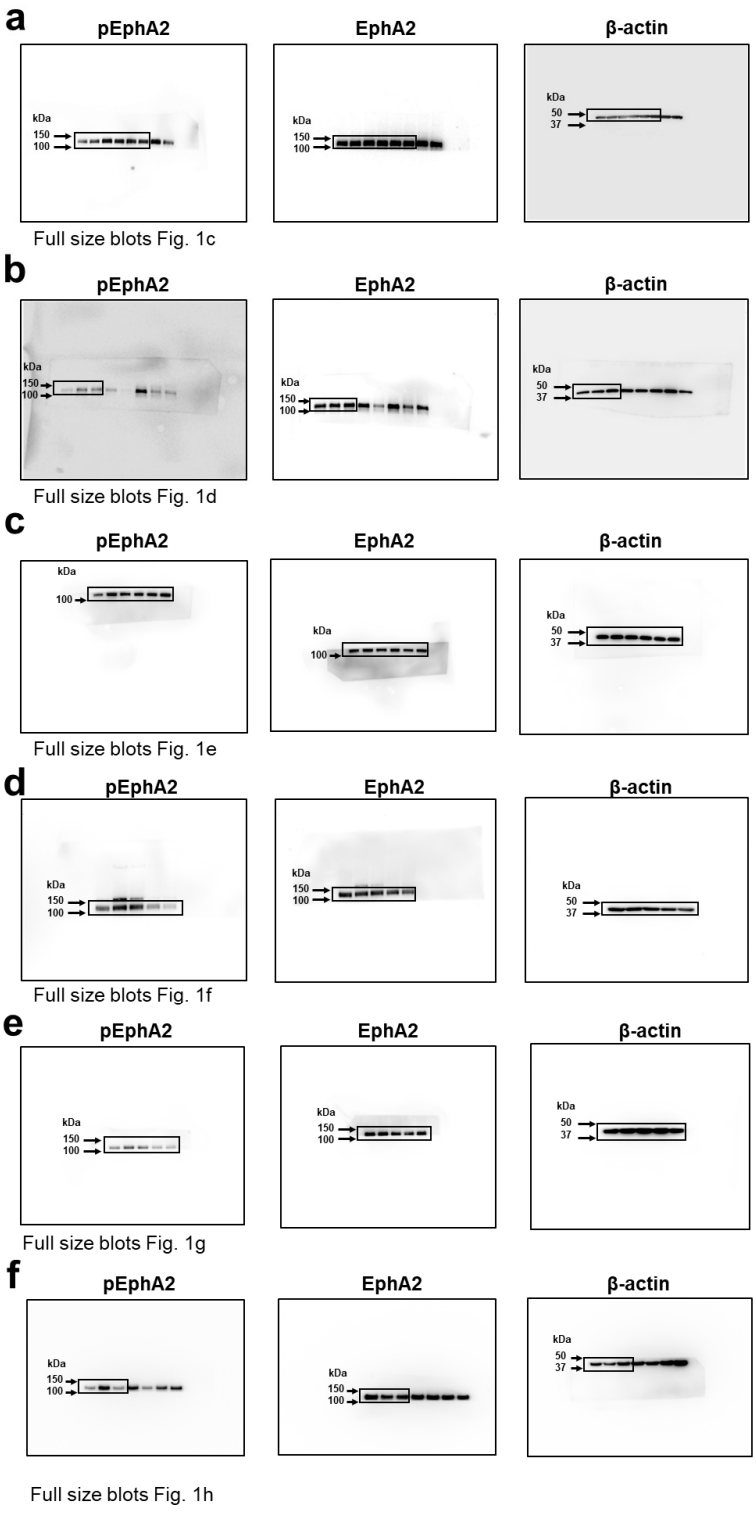

Supplementary Figure 27 Full size blots of Fig.1.

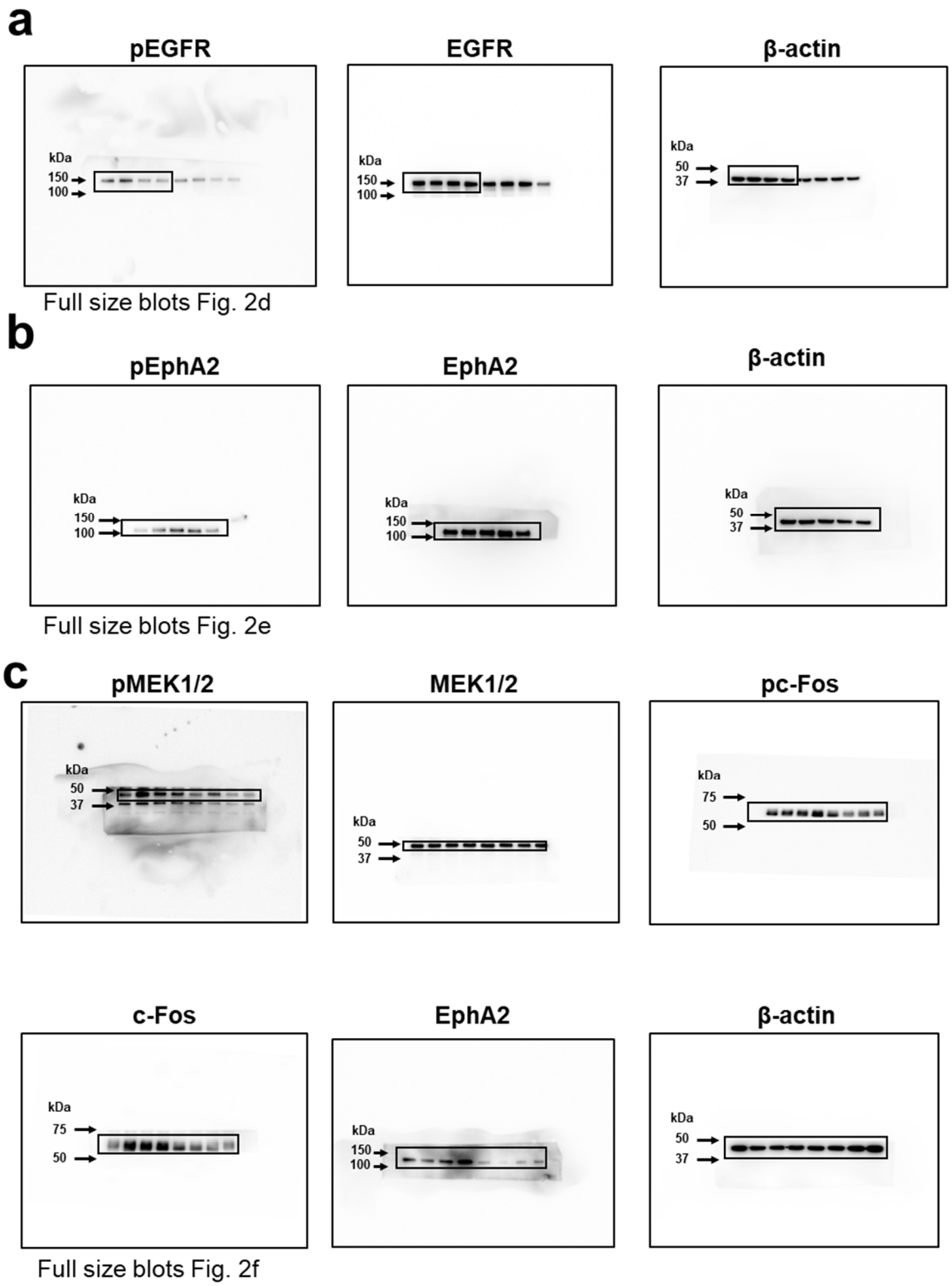

Supplementary Figure 28 Full size blots of Fig.2d-f.

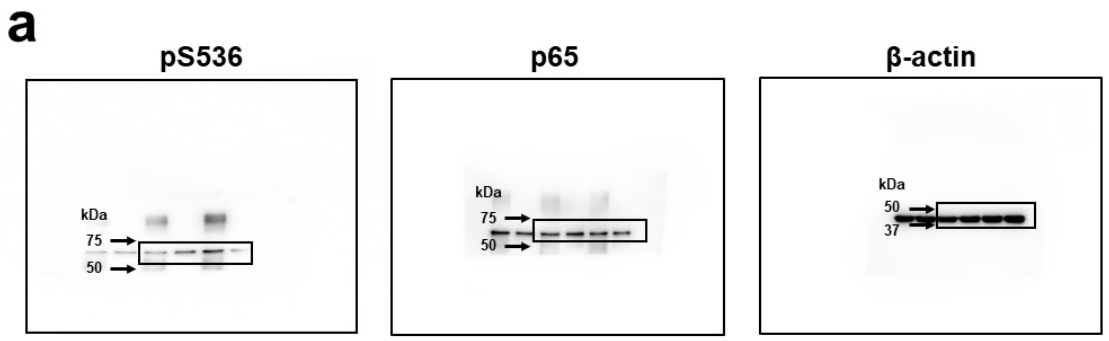

Full size blots Fig. 2g

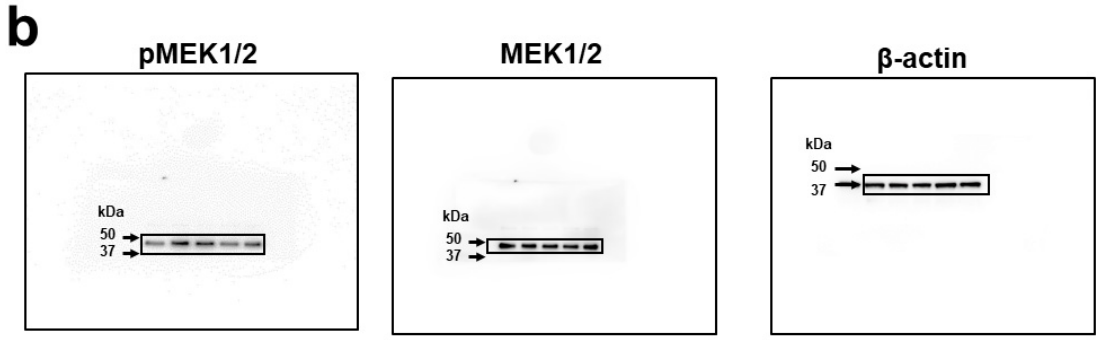

Full size blots Fig. 2h.

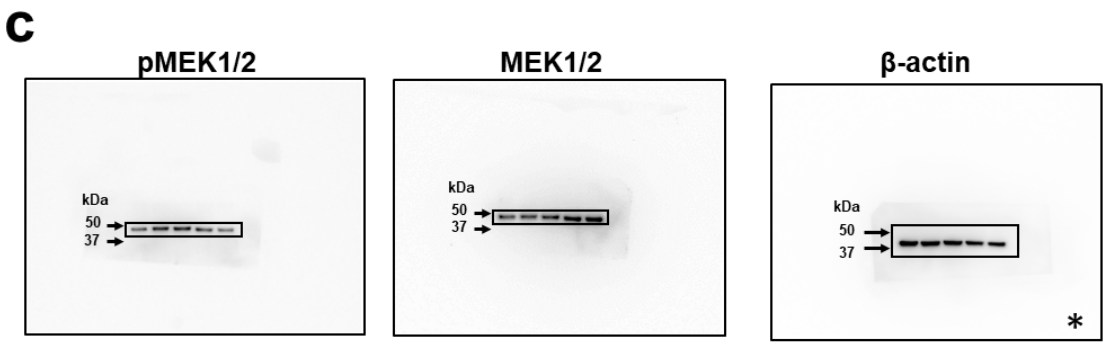

Full size blots Fig. 2i. * same β-actin immunoblot as in Fig 2e.

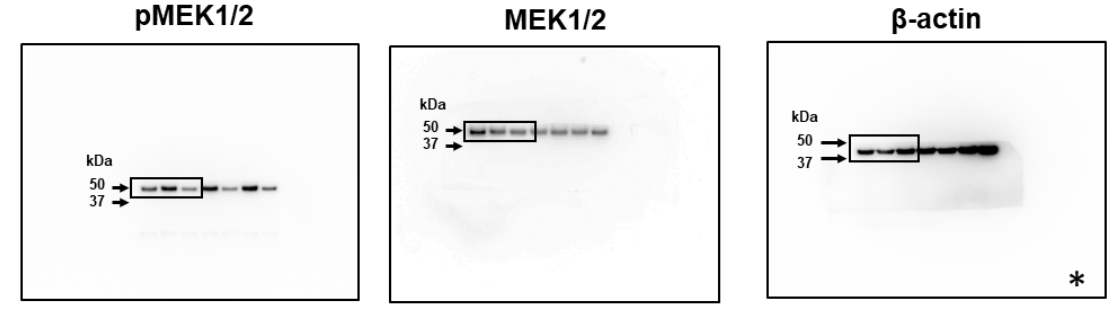

Full size blots Fig. 2j. * same β-actin immunoblot as in Fig. 1f.

Supplementary Figure 29 Full size blots of Fig.2g-j.

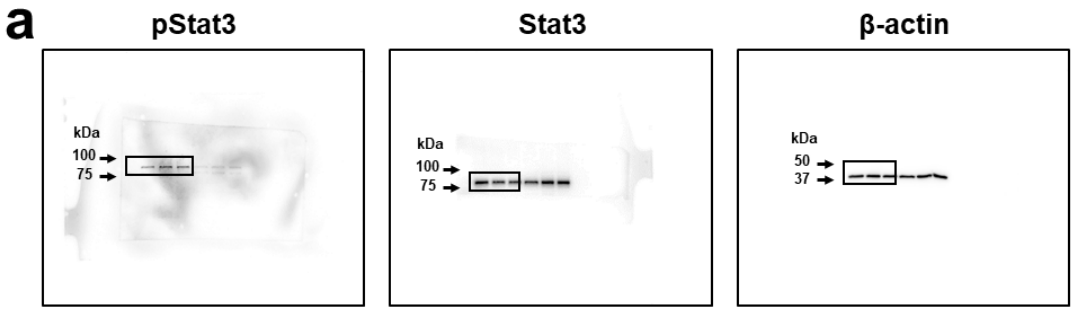

Full size blots Fig. 3a

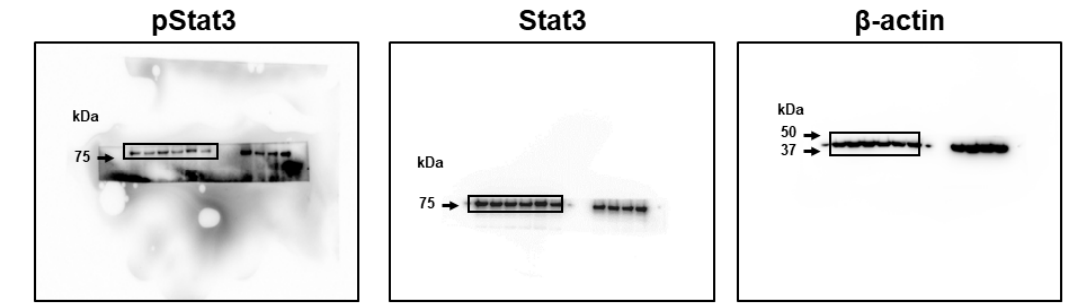

Full size blots Fig. 3b

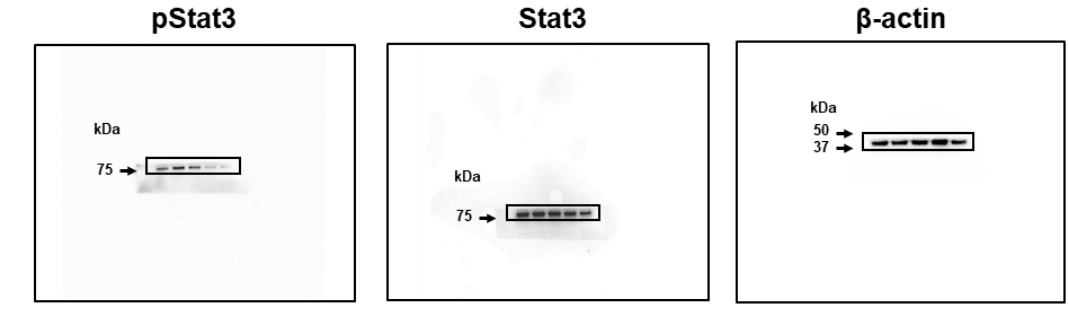

Full size blots Fig. 3c

Supplementary Figure 30 Full size blots of Fig.3.

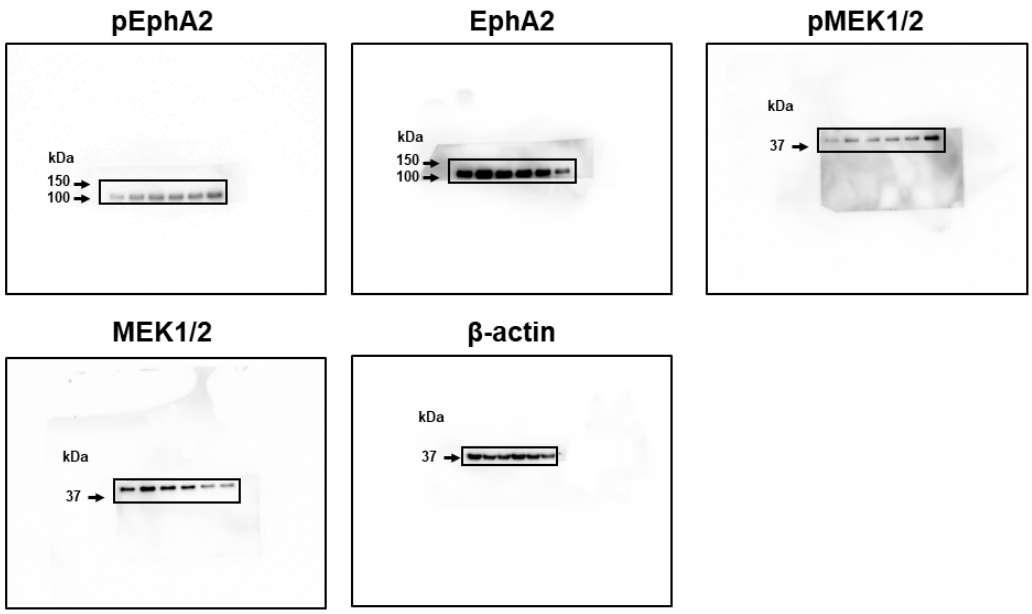

Full size blots Fig. 4a

Supplementary Figure 31 Full size blots of Fig.4.

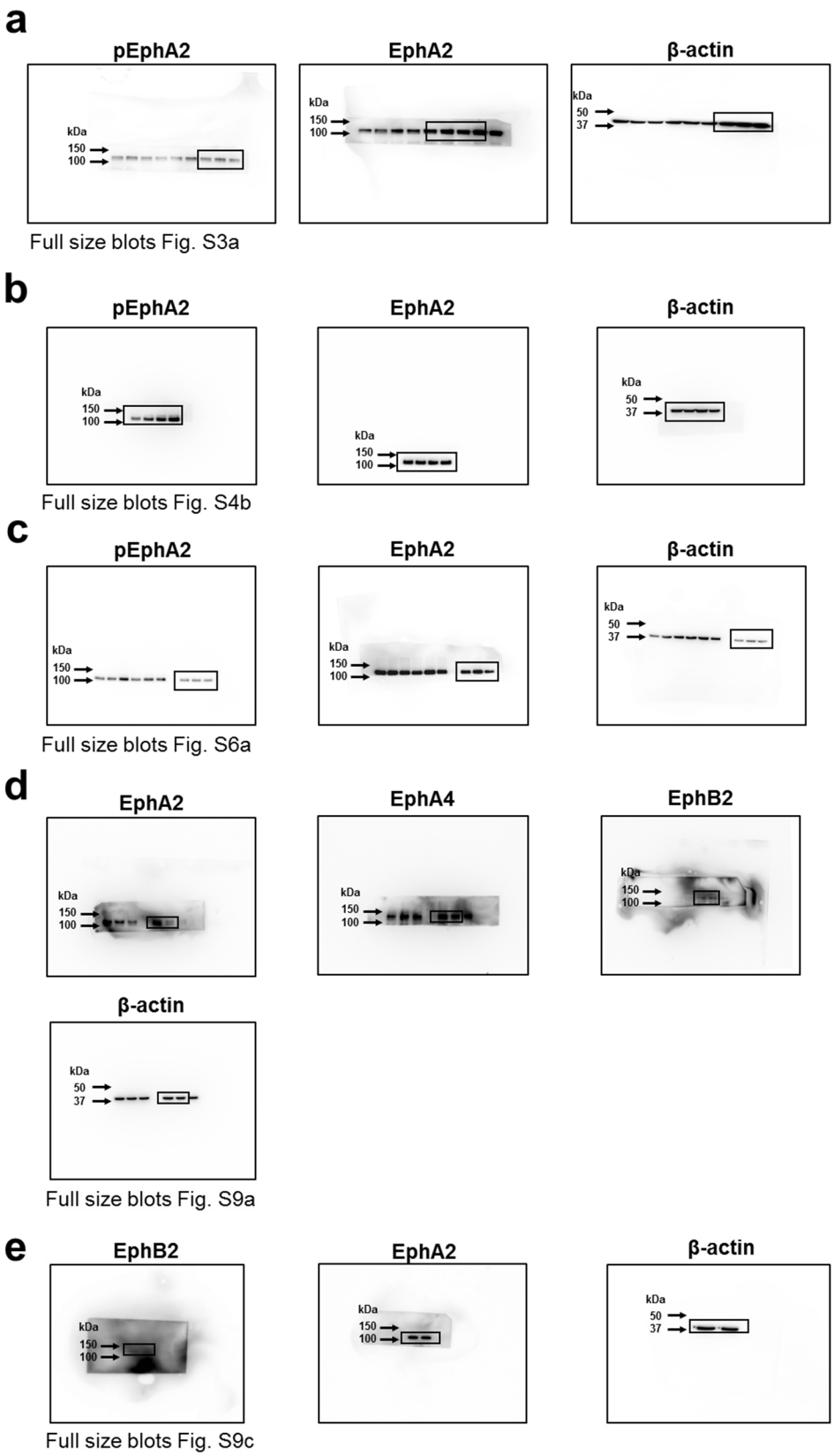

Supplementary Figure 32 Full size blots of Fig. S3a, S4b, S6a, S9a, and S9c.

Full size blots Fig. S10a

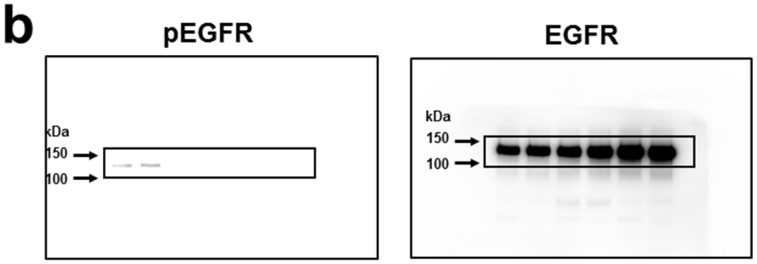

Full size blots Fig. S12b

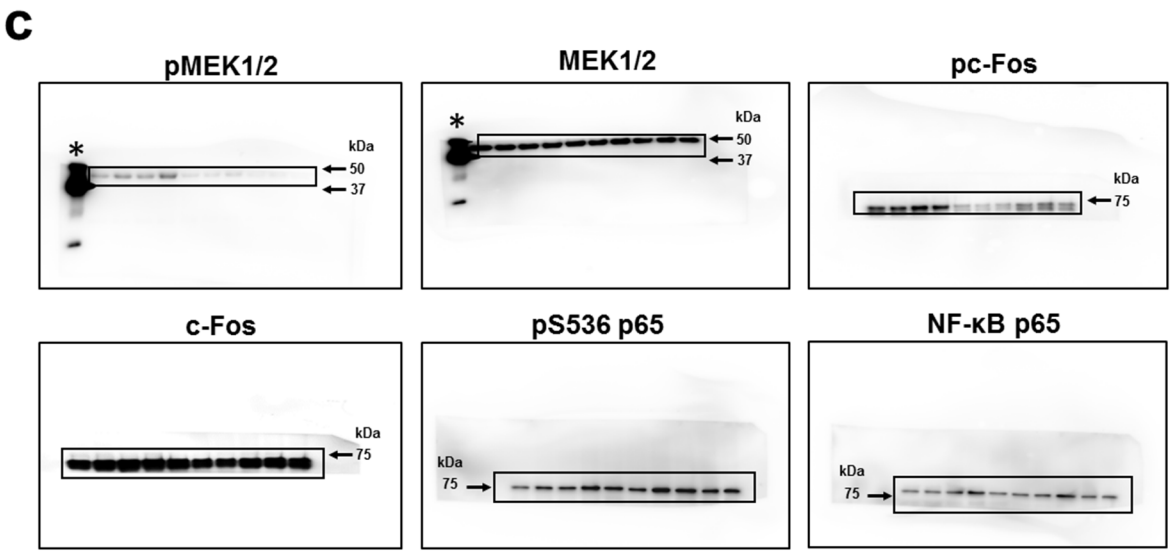

Full size blots Fig. S13b. * unspecific marker bands.

Full size blots Fig. S16a. Same immunoblots as in Fig. S6a.

Supplementary Figure 33 Full size blots of Fig. S10a, S12b, S13b, and S16a.

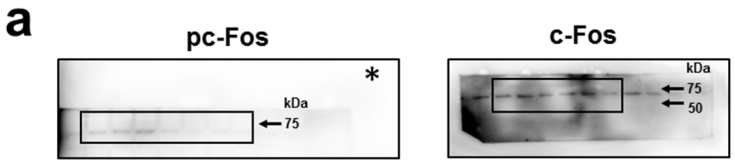

Full size blots Fig. S17a. *defined area was exposed to decrease background.

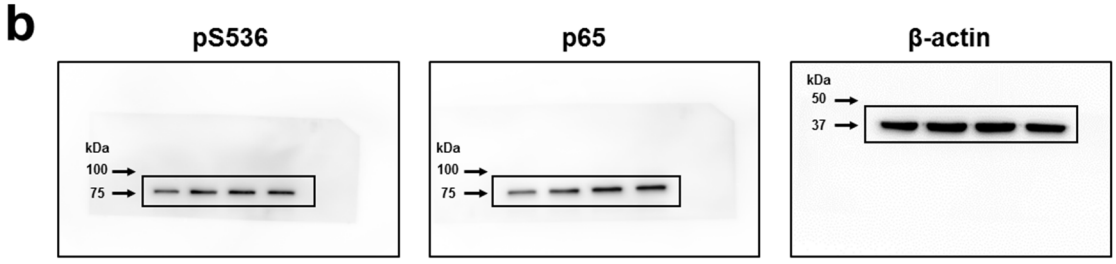

Full size blots Fig. S17c

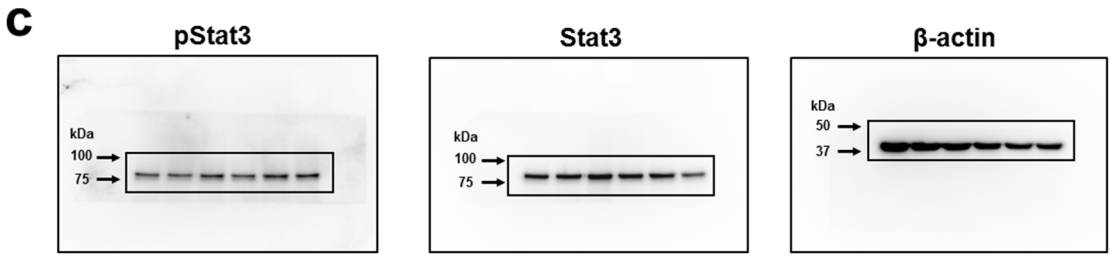

Full size blots Fig. S20a

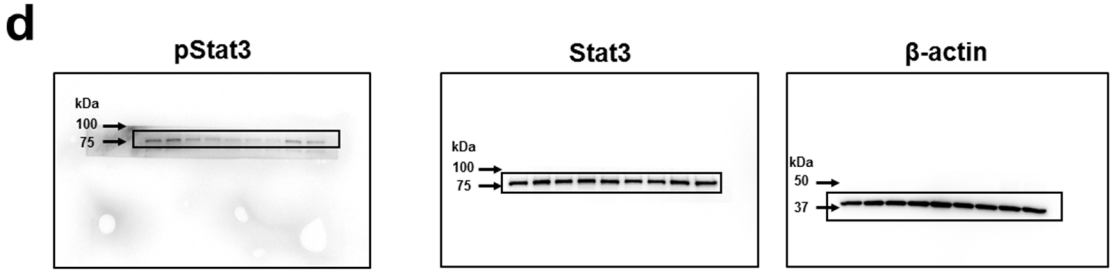

Full size blots Fig. S20c

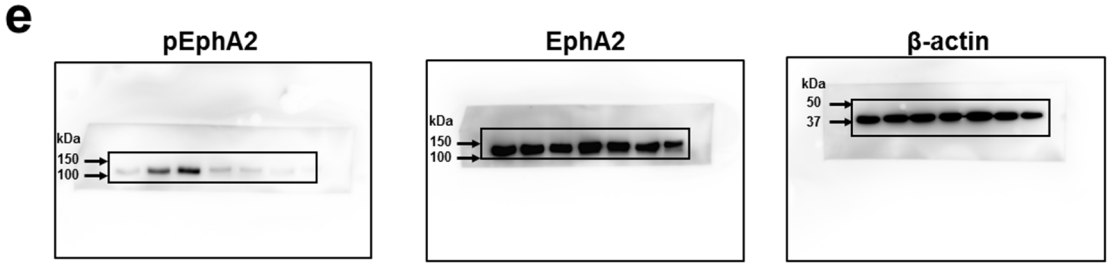

Full size blots Fig. S23c

Supplementary Figure 34 Full size blots of Fig. S17a, S12c, S20a, S20c and S23c.

Supplementary references

1 Fonzi, W. A. & Irwin, M. Y. Isogenic strain construction and gene mapping in *Candida albicans*. *Genetics* **134**, 717-728 (1993).

2 Alarco, A.-M. *et al.* Immune-deficient *Drosophila melanogaster*: a model for the innate immune response to human fungal pathogens. *J. Immunol.* **172**, 5622-5628 (2004).

3 Rahman, D., Mistry, M., Thavaraj, S., Challacombe, S. J. & Naglik, J. R. Murine model of concurrent oral and vaginal *Candida albicans* colonization to study epithelial host-pathogen interactions. *Microbes Infect.* **9**, 615-622 (2007).

4 Lo, H. J. *et al.* Nonfilamentous *C. albicans* mutants are avirulent. *Cell* **90**, 939-949 (1997).

5 Sun, J. N. *et al.* Host cell invasion and virulence mediated by *Candida albicans* Ssa1. *PLoS Pathog.* **6**, e1001181 (2010).

6 Moyes, D. L. *et al.* Candidalysin is a fungal peptide toxin critical for mucosal infection. *Nature* **532**, 64-68 (2016).

7 Wiederhold, N. P. *et al.* In vivo efficacy of anidulafungin and caspofungin against *Candida glabrata* and association with in vitro potency in the presence of sera. *Antimicrob. Agents Chemother.* **51**, 1616-1620 (2007).

8 Brachmann, C. B. *et al.* Designer deletion strains derived from *Saccharomyces cerevisiae* S288C: a useful set of strains and plasmids for PCR-mediated gene disruption and other applications. *Yeast* **14**, 115-132 (1998).

9 Ma, L. J. *et al.* Genomic analysis of the basal lineage fungus Rhizopus oryzae reveals a whole-genome duplication. *PLoS Genet.* **5**, 3 (2009).

10 Nierman, W. C. *et al.* Genomic sequence of the pathogenic and allergenic filamentous fungus *Aspergillus fumigatus*. *Nature* **438**, 1151-1156 (2005).

11 Baker, T. A., Grossman, A. D. & Gross, C. A. A gene regulating the heat shock response in *Escherichia coli* also affects proteolysis. *Proc. Natl. Acad. Sci. USA* **81**, 6779-6783 (1984).

12 Horsburgh, M. J. *et al.* σB modulates virulence determinant expression and stress resistance: characterization of a functional rsbU strain derived from *Staphylococcus aureus* 8325-4. *J. Bacteriol.* **184**, 5457-5467 (2002).